ESRF	**Experiment title:** **Exploring the competition of antiferrodistorsive and polar instabilities in $Ba_{1-x}Eu_xTiO_3$ system using powder diffraction**	**Experiment number**: CH-4799
Beamline: ID22	**Date of experiment**: from: 15/02/2017 to: 21/02/2017	**Date of report**: 21.03.2017
Shifts: 18	**Local contact(s)**: CODURI Mauro	*Received at ESRF:*

Names and affiliations of applicants (* indicates experimentalists):

Marco Scavini*, Carlo Castellano, Stefano Checchia*, Mattia Allieta
Università degli Studi di Milano, Dip. di Chimica, Milano, Italy;

Xingxing Xiao, Marc Widenmeyer*, Songhak Yoon, Tobias Kohler*, Anke Weidenkaff
University of Stuttgart, Institute for Materials Science, Heisenbergstr. 3, 70569 Stuttgart, Germany

Mauro Coduri*, ESRF

Report:.

Combining the polar displacements and octahedra tilting of the ferroelectric $BaTiO_3$ and magnetoelectric $EuTiO_3$, the $Ba_{1-x}EuTiO_3$ (BETO) solid solution displays very interesting physical properties, as recently shown in Ref.[1].

In experiment CH4799, we measured accurately the structure of BETO at long, medium, and short length scales, as a function of both temperature and composition, by means of high resolution powder diffraction measurements coupled with the real-space Pair Distribution Function (PDF) analysis.

Samples

Samples of $Ba_{1-x}Eu_xTiO_3$ (x = 0.05, 0.15, 0.20, 0.3, 0.5, 0.7, 0.8, 0.9, 1.0) were prepared using a Pechini method followed by annealing and sintering under reducing conditions at 1273 K, as described in Ref.[1]. Two compositions (x = 0.05 and 0.15) were additionally annealed at 1473 K.

Data collection strategy

XRPD data were collected at the ID22 beamline selecting an X-ray wavelength of λ = 0.335014(5) Å and using a 9-elements detector array (high resolution setup). Powdered samples of BETO were cooled down to 10 K in a He-cryostat and PDF-quality patterns were collected up to $Q_{max} \approx 26$ Å^{-1}. Next, samples were heated to 150 K with an heating rate of 1 K/min while Rietveld quality patterns were collected up to Q_{max}= 14 Å^{-1} at fixed temperature values (T = 30, 50, 70, 90, 120, 150 K). In addition, samples with x = 0.05 and 0.15 fired at 1473 K, were measured at 120, 200, 250, 300, 350 and 400 K using the cryostream for heating.

Fast patterns (60 seconds) were also collected continually during all temperature ramps.

Results:

All solid solution prepared at 1273 K are cubic down to 10 K. In figure 1 the Rietveld refinements of the samples x = 0.05 and x = 0.80 using the cubic perovskite structural model (space group *Pm*-3*m*) are shown as examples.

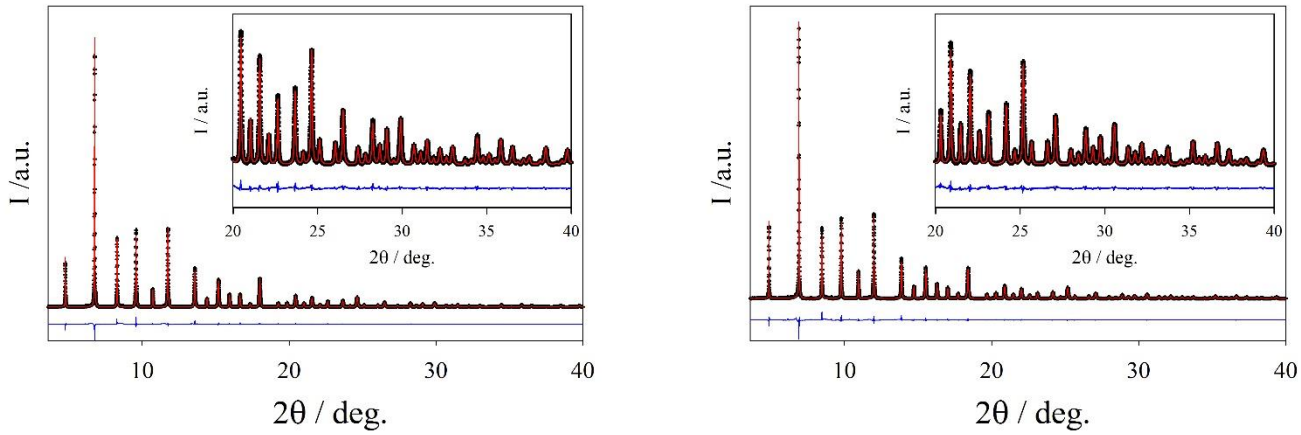

Figure 1. Rietveld refinements of XRPD patterns collected at 10 K on $Ba_{1-x}Eu_xTiO_{3-\delta}$ samples annealed at 1273 K with x = 0.05 (left) and x = 0.80 (right). Experimental data (black symbols) are shown together with the fit (red lines) and the residuals (blue lines). The insets report the high 2θ angle range of the refinements.

Preliminary Rietveld analysis revealed a complex behaviour of the atomic mean square parameters *U* (Figure 2). The bell shaped dependence of *U*(O) on composition matches the positional disorder induced by the Eu/Ba mixing at the *A*-site with fluctuations expected in Eu/Ba-O interatomic distances. Differently, *U*(Ti) decreases monotonically by increasing Eu^{2+} concentration and for Ba-rich samples, particularly for x = 0.05, *U*(Ti) is three times larger as *U*(Ba/Eu), suggesting a local polar distortion of Ti atoms within the overall cubic structure.

The Williamson-Hall size/strain analysis revealed the presence of a very huge strain (quantified by the strain parameter $\varepsilon = \Delta a/a$) for intermediate compositions.

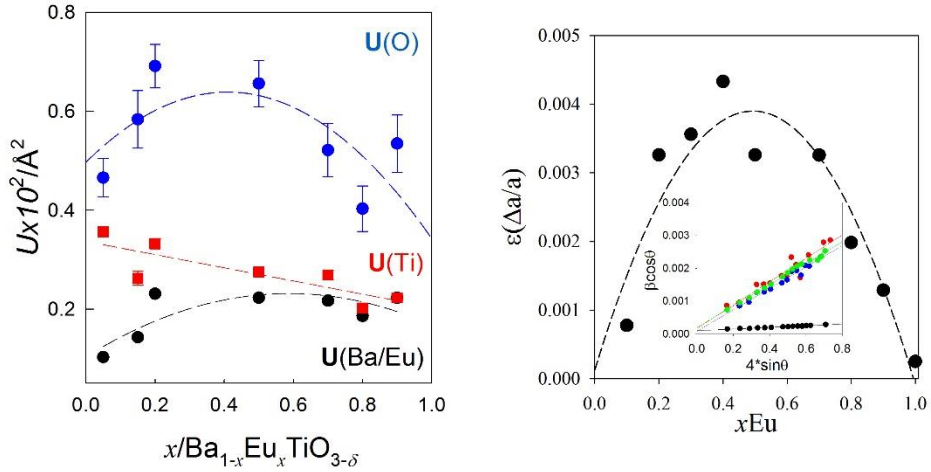

Figure 2.
$Ba_{1-x}Eu_xTiO_{3-\delta}$ samples at 10 K.
Left. Atomic mean square parameters *U*
Right. Strain parameter ε as extracted by Williamson-Hall analysis. The inset reports selected WH fits pertinent to $EuTiO_3$ (black circles) and to x = 0.3, 0.5, 0.7 solid solutions (red, green and blue circles).
In all the figures, dashed lines are guides for the eyes.

Unlike any of the samples prepared at 1273 K, solid solutions with x = 0.05 and 0.15 sintered at 1473 K were rhombohedral (space group *R*3*m*) at 10 K. On heating up to 400 K, these two samples underwent all the phase transitions typical for $BaTiO_3$ [2]: i) to orthorhombic *Amm*2; ii) to tetragonal *P*4*mm* space group and, finally, iii) to cubic *Pm*-3*m* space group. Figure 3 shows as examples the patterns at 10 K (space group *R*3*m*) and 400 K (space group *Pm*-3*m*) of $Ba_{0.85}Eu_{0.15}TiO_{3-\delta}$ prepared at 1473 K.

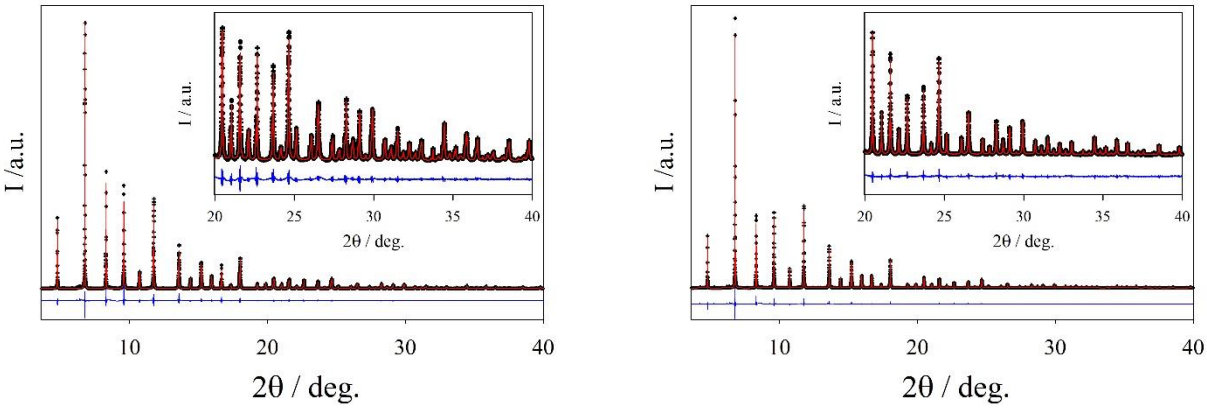

Figure 3. XRPD patterns collected on $Ba_{0.85}Eu_{0.15}TiO_{3-\delta}$ sample annealed at 1473 K. Rietveld refinements of at 10 K (left) and 400 K (right) using rhombohedral and cubic structural models, respectively. Experimental data (black symbols) are shown together with the fit (red lines) and the residuals (blue lines). The insets report the high 2θ angle range.

The short- and medium-range structures are being studied by means of PDF analysis through the G(*r*) function. Analysing G(*r*) curves for different compositions in a wide range of interatomic distances allows understanding both nature and coherence length of distortions induced by the different chemical environments of Ba and Eu. To aid in this understanding, EXAFS measurements on the same samples (taking place at BM23 in early April [3]) will discriminate the specific contributions of Ba and Eu to the short-range structure.

Comparing the G(*r*) of pairs of samples with the same composition, but annealed at different temperatures highlights their structural contrasting behaviour at low *T* values, as noted above when discussing phase transitions. Figure 4 shows selected ranges of the experimental G(*r*) of samples $x = 0.05$ (top panel) and $x = 0.15$ (bottom panel) annealed at 1273 (black curves) and 1473 K (red curves). At low *r*, differences between samples annealed at different temperatures are negligible and all curves can be fitted using the same rhombohedral structural model describing the average structure of the 1473 K annelaed sample at the same temperature (10 K).

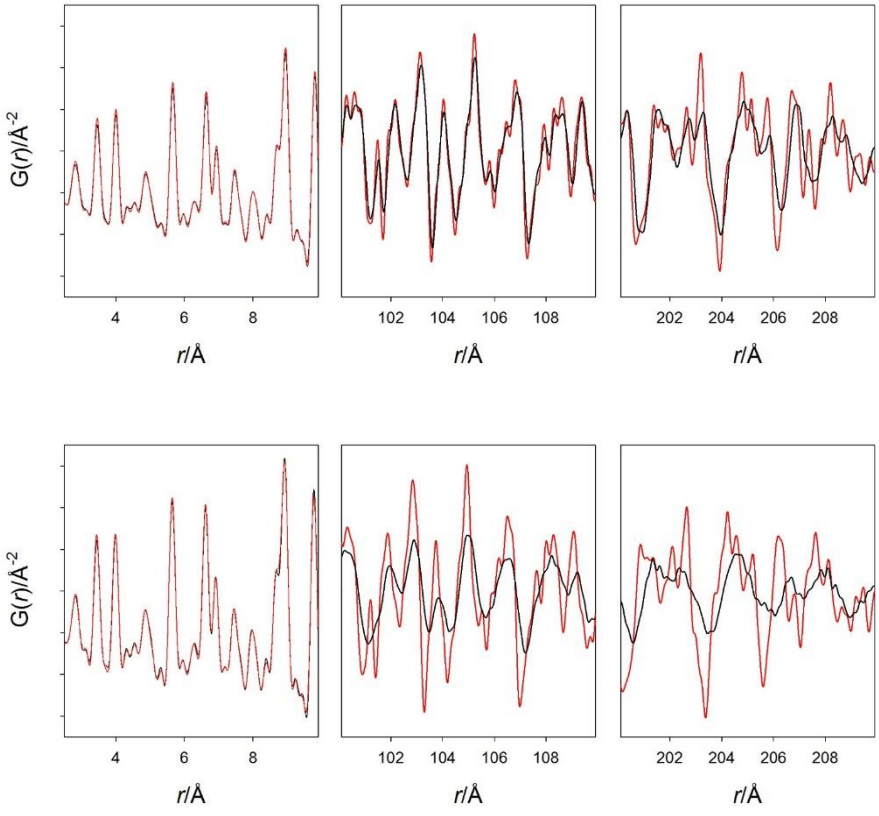

Figure 4.

Portions of G(*r*) functions at 10 K of $Ba_{1-x}Eu_xTiO_{3-\delta}$ samples with $x = 0.05$ (up) and $x = 0.15$ (down) prepared at 1273 K (black lines) and 1473 K (red lines). Y axes in panels at different *r* ranges have different amplitudes.

Figure **5** shows the fits of G(*r*) curves at low *r* values related to *x* = 0.05 and 0.15 samples annealed at 1273 K. The low fit residuals (R_W) signal a good agreement with the local *R*3*m* space group despite their average cubic structure. The G(*r*) curves of samples with the same composition and different annealing temperatures only become different in a further *r* range (see Fig. 4). In particular, the G(*r*) peaks of the samples annealed at 1273 K are visibly smeared compared with those of the samples annealed at 1473 K, suggesting smaller crystallite coherence length and/or increased disorder. Also, while for samples annealed at 1473 K the coherence length of rhombohedral domains seems to be hardly affected by sample composition, the G(*r*) peaks of the samples annealed at 1273 K clearly broaden with increasing Eu concentration, suggesting that the structural order is a complex function of the annealing temperature and composition.

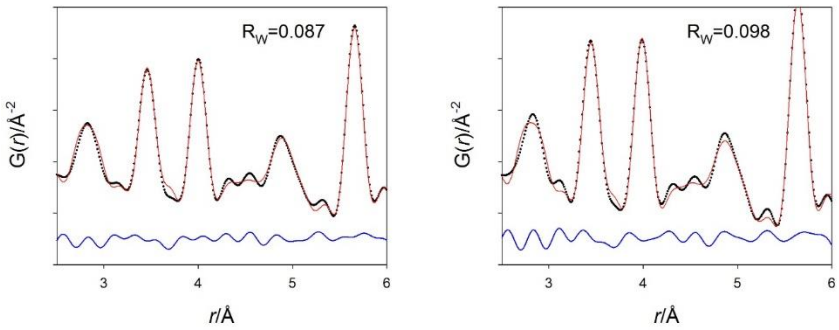

Figure 5.

Fit of G(*r*) functions at 10 K of $Ba_{1-x}Eu_xTiO_{3-\delta}$ samples prepared at 1273 K with *x* = 0.05 (left) and *x* = 0.15 (right) using the rhombohedral *R*3*m* structural model. Experimental data (black symbols) are shown together with the fit (red lines) and the residuals (blue lines).

Outlooks and future developments

The formidable *Q*-resolution of the ID22 beamline makes it possible to study the structure of BETO solid solutions at different length scales, which is of extreme importance to fully understand the (thermal) transport properties of these thermoelectric materials. On one hand, the electronic structure should be strictly related to the crystallographic short range structure and band calculations based only on the average cubic structure should be inaccurate. On the other hand, charge and heat transport should be affected by the local structure, the degree of disorder, and the way the local rhombohedral domains merge into the average structure, e.g. by the coherence length of *R*3*m* domains which, as shown above, depends on both composition and sintering temperature.

In a recently submitted beamtime proposal we plan to measure more accurately samples in the Ba-rich part of the phase diagram (*x* = 0.05, 0.10, 0.15, 0.20, 0.25, 0.30), where local rhombohedral domains dominate the short-range BETO structure. High resolution experiments will be performed on samples annealed at different temperatures. In fact, laboratory XRPD measurements at room temperature showed that samples with *x* > 0.15 annealed at 1473 K are cubic, while annealing at 1673 K results in a tetragonal structure. High resolution XRPD data will be taken from 10 K to above the tetragonal-cubic phase transition (300-400 K, depending on the sample).

References

[1] X. Xiao, M. Widenmeyer, M. Scavini, A.Weidenkaff, et al. *Phys. Chem. Chem. Phys.*, 2017, in press. DOI: 10.1039/C7CP00020K

[2] G.H. Kwei, A.C. Lawson, S. J. L. Billinge S.-W. Cbeong J. Phys. Chem. 1993, **97**, 2368-2377

[3] Experiment CH-5039 at the BM23 beamline of the ESRF, 06-11.04.2017